Rapid and controllable sintering of gold nanoparticle inks at room temperature using a chemical agent

By *Michael J. Coutts*, *Michael B. Cortie*, *Michael J. Ford*, *and Andrew M. McDonagh**

Institute for Nanoscale Technology, University of Technology Sydney, Broadway Sydney NSW 2007 Australia. Fax: (+61) 2 9514 1460

E-mail: andrew.mcdonagh@uts.edu.au

We show that oxidation of protective thiol ligands and the exothermic reduction of surface area are important factors in the sintering of thiol-stabilized gold nanoparticle films. We also present a chemical treatment to achieve sintering of gold nanoparticles at room temperature. The process is facilitated by the remarkable enthalpy of reaction arising from the reduction of the surface area of the nanoparticles.

Keywords: gold, nanoparticles, sintering, thiols

Introduction

Films of thiol-stabilized gold nanoparticles are generally not very conductive, but after sintering their conductivity is comparable to that of bulk gold.[1] Sintering of gold nanoparticles is an attractive technique for the fabrication of low cost printable electronic devices such as thin-film transistors,[1] field effect transistors,[2, 3] contacts,[1, 3-5] and conducting wires.[6, 7] Tracks can be printed to the required dimensions and the whole item heated to achieve sintering, or they may be selectively heated (and thus sintered) by rastering with a laser of sufficient power,[8] or the desired metallic regions may be defined using UV photolithography.[9] Here we demonstrate a means to achieve sintering of gold nanoparticles at *room temperature* using a simple chemical treatment. The process is facilitated by the remarkable enthalpy of reaction which arises from the reduction of the surface area of the nanoparticles. The innovation may permit the full flexibility of ink-jet printed electronic circuitry to be unlocked, even on temperature sensitive substrates.

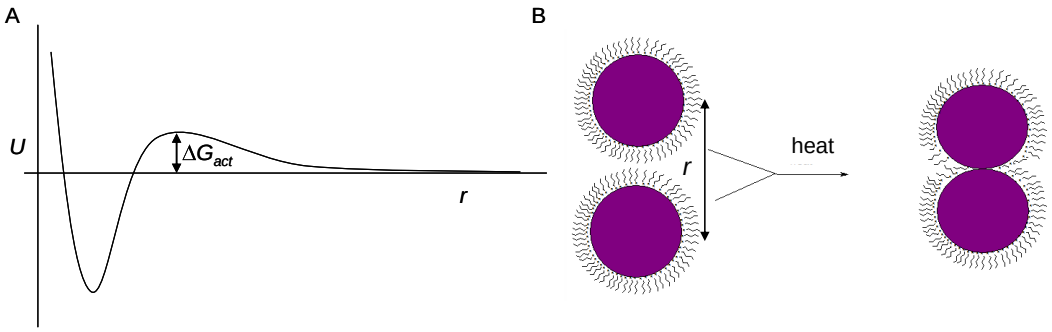

Figure 1. A. Potential energy (U) curve representing the interaction of stabilized gold nanoparticles separated by a distance, r. B. Schematic representation of the sintering of two gold nanoparticles.

Thiol-stabilized particles are commonly used in these products due to their solubility in organic solvents and the moderate temperatures (~200 °C) required for reasonably rapid sintering. A gold nanoparticle ink that could be sintered at as low as 140ºC has been reported.[1] In contrast, the decorative gold glazes used in the ceramics industry generally require temperatures of above 500 ºC to achieve

sintering.[10] The stabilising ligands, which provide an energy barrier to sintering, generally consist of two parts; the anchoring group, which forms a sulfur-gold bond to the particle surface, and the separating component, which can vary from alkane chains to aromatic structures or even polymers. Particles will sinter if the thermal energy of the system is sufficient to overcome the activation energy, ΔG_{act}, provided by the stabilising ligand (Figure 1). Sintering of a collection of many particles will result in the formation of a relatively continuous gold film.

Molecular dynamics simulations[11, 12] and experimental results[5] show that nanoparticles sinter via a "necking" mechanism where two particles first join together to form a peanut-like shape before the surface area is minimised and larger particles form. Calculations indicate that heat is released as a result of the surface area minimisation,[11, 12] however this has not been previously confirmed experimentally. So while thermodynamically favourable, sintering is dependent on kinetics and in particular on ΔG_{act}. We note that while sintering may be performed at a particular temperature, there is no formal "sintering temperature" in the same sense that materials have specific melting points. This is because sintering is a thermally activated phenomenon and so the term "sintering temperature" is unhelpful in the context of the current work. Mechanistic discussion should rather focus on a rate of sintering.

Huang *et al.*[4] proposed that the sintering of thiol-stabilised gold nanoparticles occurs in two steps where the organic stabilising ligand first sublimates and the nanocrystals then fuse becoming electrically conductive. Subsequently, Wu *et al.*[1] showed using thermogravimetric analysis (TGA) that weight loss occurs upon heating gold nanocrystals, this loss is reasoned to be the removal of the organic stabilising ligand. In these previous studies and in the current work, the temperatures used for sintering are well below the melting points of the gold nanoparticles being investigated.[13, 14]

Experimental

General. MilliQ water (18 MΩ cm^{-1}) was used in synthetic procedures. Tetrachloroauric acid was prepared using a literature procedure.[15] 1-Butanethiol (Aldrich), tetraoctylammonium bromide (Aldrich), toluene, sodium borohydride, sodium sulphate, cyclohexane, methanol, dichloromethane, nitric acid

were all used as received. NO_2 gas was generated by dropping concentrated nitric acid onto copper turnings and mixing the collected gas with air prior to directing it onto the nanoparticle films.

Synthesis of gold nanoparticles. 1-alkanethiol-stabilised gold nanoparticles where synthesised by the method described by Wu *et al.*[1] The particles were characterized by UV-visible spectroscopy and scanning electron microscopy.

Physical measurements. UV-visible spectra of the particles in dichloromethane were recorded using a Shimadzu Mini UV 1240 spectrophotometer. SEM images where obtained using a LEO Zeiss Supra 55VP Scanning Electron Microscope operating in high vacuum mode. Films were deposited on a 2 cm x 2 cm square of indium tin oxide coated glass. TGA experiments where performed using SDT 2960 and SETARAM setsys TG-DSC 15 instruments with simultaneous DSC-TGA. Heating rates of 0.5 $^{o}C\ min^{-1}$ to 5 $^{o}C\ min^{-1}$ where used in air, nitrogen and Ultra High Purity (UHP) argon atmospheres.

For resistance measurements, two 100 nm thick gold electrodes separated by a gap of 200 μm where fabricated on a glass slide that was cleaned by sonication in a detergent solution for 10 min followed by thorough rinsing with MilliQ water and drying in a stream of nitrogen. Vacuum deposition was performed using a Denton bell jar DV-502 vacuum chamber where gold was thermally evaporated on a tungsten filament operating at ~20 A resulting in a deposition rate of between 1 and 2 $Å\ s^{-1}$. A 200 μm gap between the gold electrodes was obtained using enamel-coated copper wire as a mask. The deposition rate, along with the film thickness was measured with a Maxtek TM-100 film thickness monitor with quartz detector. The separation distance between the electrodes was determined using an optical microscope camera setup with calibrated imaging software. A 4 μL drop of a gold nanoparticle solution (10 mg of gold nanoparticles in 200 μL of dichloromethane) was deposited such that it spanned the electrode gap. We note that variation in drop volume (up to 8 μL) gave no variation in sintering rate. A k-type thermocouple was attached to the sample, which was then heated on a heating stage. The heating rate was constant throughout a given experiment. Resistance as a function of temperature was recorded using a customised LabVIew program utilising two Yokogowa 7562 digital multimeters for

temperature/resistance measurements and a Yokogowa 7651 programmable DC power source/relay setup to control a variable voltage transformer attached to a heat stage.

Results and discussion

Scanning electron microscope images of 1-butanethiol-stabilized gold nanoparticles show that when deposited as a film, the particles are discrete and relatively monodisperse with a diameter of ~4 nm (see Figure 2). After sintering, the films no longer contain discrete particles but instead are continuous in nature.

The conductivities of films of gold nanoparticles were measured as a function of temperature using two gold electrodes on glass separated by a distance of 200 μm. A thin film of gold nanoparticles spanning the electrodes was deposited from dichloromethane solution and the resistance measured while the film was heated. Figure 2A shows film resistance as function of temperature for a linear temperature ramp of ~5 K min^{-1}. The initial resistance of 10-12 MΩ gradually decreased as the particles were heated until the temperature reached ~150 ^{o}C whereupon the resistance dropped rapidly to 2-5 Ω. This change in resistance occurs in conjunction with a colour change from brown/black to gold and corresponds to the sintering process. The previously reported dependence of sintering on alkane chain length[1] suggested to us that ligand volatility might play a role in the sintering process and ligands with higher boiling points might sinter at a slower rate. Equivalently one might expect a dependence of sintering rate with pressure. We therefore heated films of 1-butanethiol-stabilised nanoparticles *in vacuo*. Surprisingly, the sintering process occurs at a much slower rate compared to atmospheric conditions and at a heating rate of 5 K min^{-1}, the dramatic conductivity change does not occur until ~220 °C (Figure 2). These results are consistent with an oxygen dependence for the sintering process. This is also consistent with the observed alkane chain length dependence noting that longer alkane chains more effectively shield the gold-thiol bond from oxygen. Interestingly, our data obtained for nanoparticles stabilized with longer alkanethiols reveals that under vacuum conditions there is a greatly reduced chain length dependence on sintering rates (see Supporting Information).

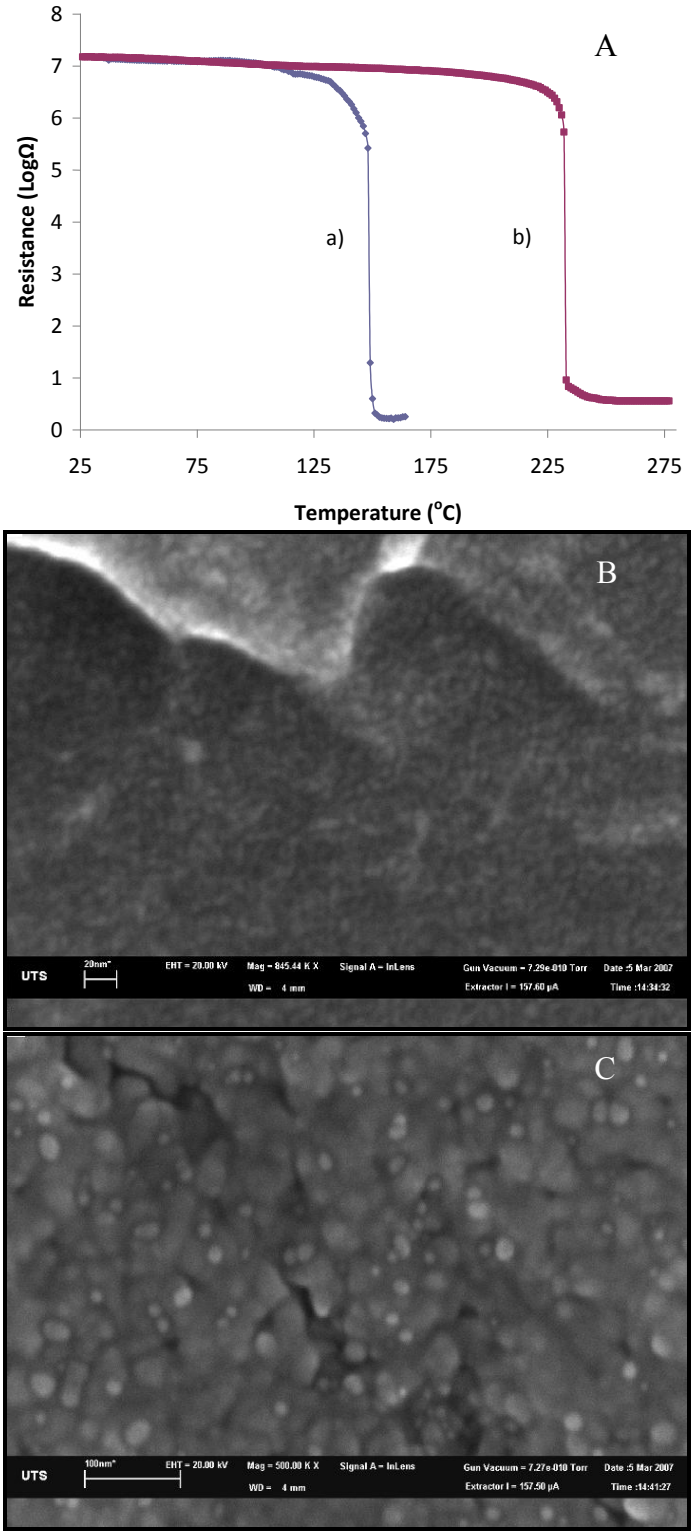

Figure 2. A) Resistance data for films of 1-butanethiol stabilized gold nanoparticles heated at 5 K min^{-1} in air, a), and *in vacuo,* b). B) SEM micrograph of 1-butanethiol-stabilised gold nanoparticles before sintering. C) SEM micrograph of 1-butanethiol-stabilised gold nanoparticles after sintering.

Thermogravimetric analysis (TGA) (Figure 3) shows that upon heating, the mass of the sample initially slowly decreases but then the rate of mass loss increases dramatically. The total mass loss is ~12.4%, which is assigned to loss of the butanethiol ligands with the remaining mass assigned to gold metal. Corresponding to the initial slow mass loss is an exothermic region in the differential scanning calorimetry data. The area under this region (~150-190 °C) of the exothermic curve yields an enthalpy of 15.3 J g^{-1}. As this region corresponds to the mass loss assigned to the butanethiol ligands, a value of ~48 kJ mol^{-1} is calculated for this process. This is followed by a remarkably sharp and large exotherm in conjunction with the rapid mass loss. We assign this feature to a surface area reduction process[16] (observed in the SEM images of films before and after sintering). We expect that pores may be present transiently between the nanoparticles during the process after ligand removal but before the surface area reduction process however *in situ* SEM imaging to examine the sintering process was not feasible. A small endothermic region is observed after this exotherm and occurs in conjunction with a continued mass loss and the sublimation of the remaining stabilising ligand.

The area under the sharp exothermic curve reveals an enthalpy of -55.75 J g^{-1}. Given that the sample consists of ~87.6 % gold by mass, the energy released from the system is 63.6 J g^{-1} (of gold) or 12.5 kJ mol^{-1}. This agrees well with the value of 10 - 12 kJ mol^{-1} calculated for 4 nm diameter spherical gold particles using a surface energy for gold[17] of ~0.7 – 0.8 Jm^{-2} and the approximation that all of the surface area is converted into heat[18] (see Supporting Information for full calculation). Assigning the exotherm to surface energy minimisation is also consistent with reported molecular dynamics calculations that indicate that heat should be released during sintering.[11, 12] It is apparent that the sintering mechanism involves an initial loss of stabilising ligands and once sufficient ligands have been removed the particles aggregate in an exothermic surface area minimisation process. At this point, a larger portion of stabilising ligand is lost and the gold forms a continuous film.

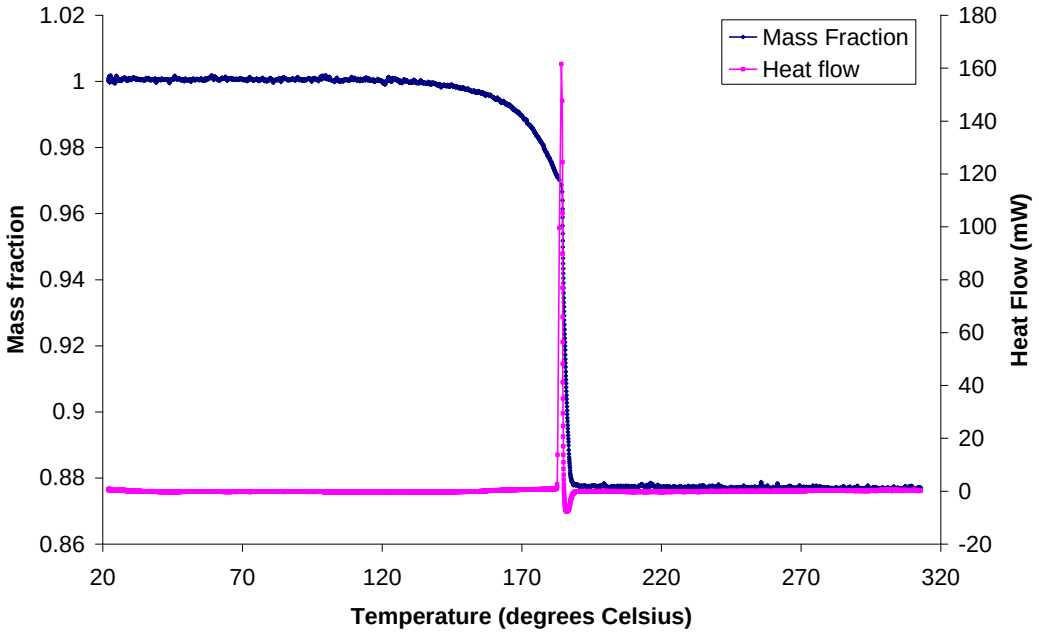

Figure 3. TGA/DSC data for 1-butanethiol-stabilised gold nanoparticles heated at 3 ^{o}C min^{-1} from room temperature to 300 ^{o}C in air.

The TGA data also provides kinetic information about the initial loss of ligands from the particles. An Arrhenius analysis of the data for different linear heating rates reveals a number of fundamental aspects of the sintering process. The relatively noisy TGA data was differentiated to determine rates of mass loss employing a Savitzky-Golay filter.[19] A zero-order rate law fits the TGA data somewhat better than other rate laws giving consistent pre-exponential factors and activation barriers. The Arrhenius analysis of the TGA data above a temperature of about 400K (0.0024 K^{-1}) and excluding the region where rapid sintering occurs (a non-equilibrium region) is shown in Figure 4. The TGA data at lower temperatures does not yield a consistent Arrhenius analysis as only very small mass loss occurs at the beginning of the TGA scan. The data for the five heating rates in Figure 4 are quite consistent and linear, indicating that there is indeed a rate limiting process with a well defined activation barrier occurring during portions of the sintering process. From the data, an activation barrier of 168 ± 15 kJ mol^{-1} is obtained. We propose that oxidation and desorption of the capping ligands accounts for this activation barrier. The observed lower sintering rate *in vacuo* and the dependence of rate upon alkane chain length supports this hypothesis. Once the thiol is oxidized, it easily desorbs from the gold surface.[20] Hence oxidation is the

rate-limiting step and the assigned order of zero in air is consistent with a constant oxygen concentration.

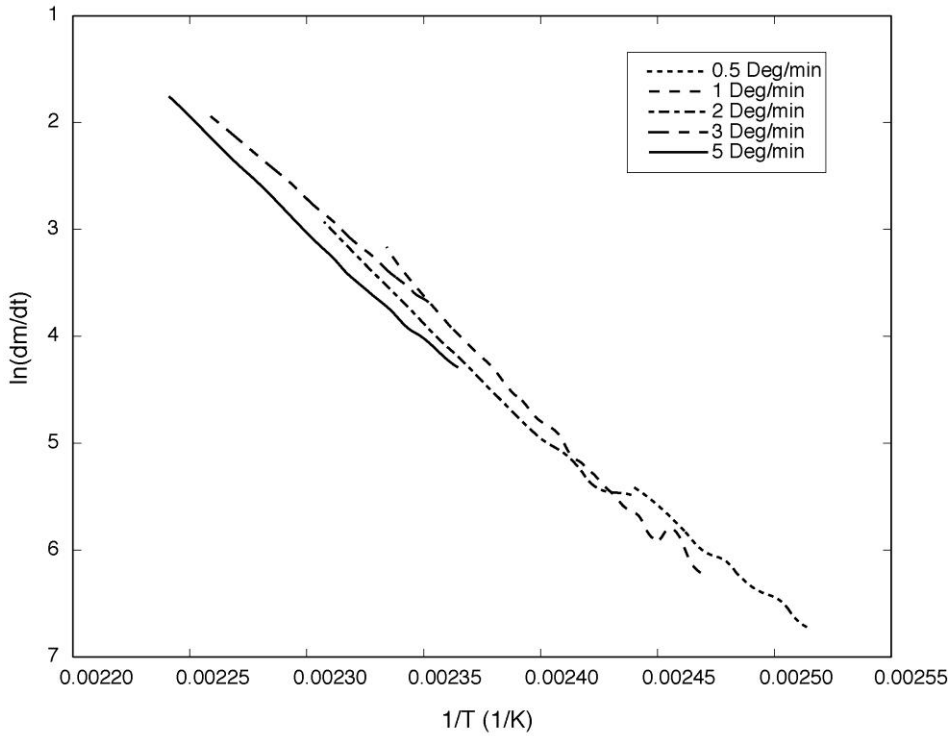

Figure 4. Arrhenius plot of the TGA data using a zero order rate law.

TGA experiments performed in an argon atmosphere show that the exothermic process occurs at a higher temperature in the atmosphere with reduced oxygen concentration upon heating at the same rate (see Supporting Information). It is also interesting to note that the exotherm occurs at approximately the same mass loss for the sample in both argon and air indicating that there is a critical level of stabilising ligand that must to be removed before sintering can occur. Clearly, decreasing the amount of oxygen in the sintering atmosphere decreases the sintering rate.

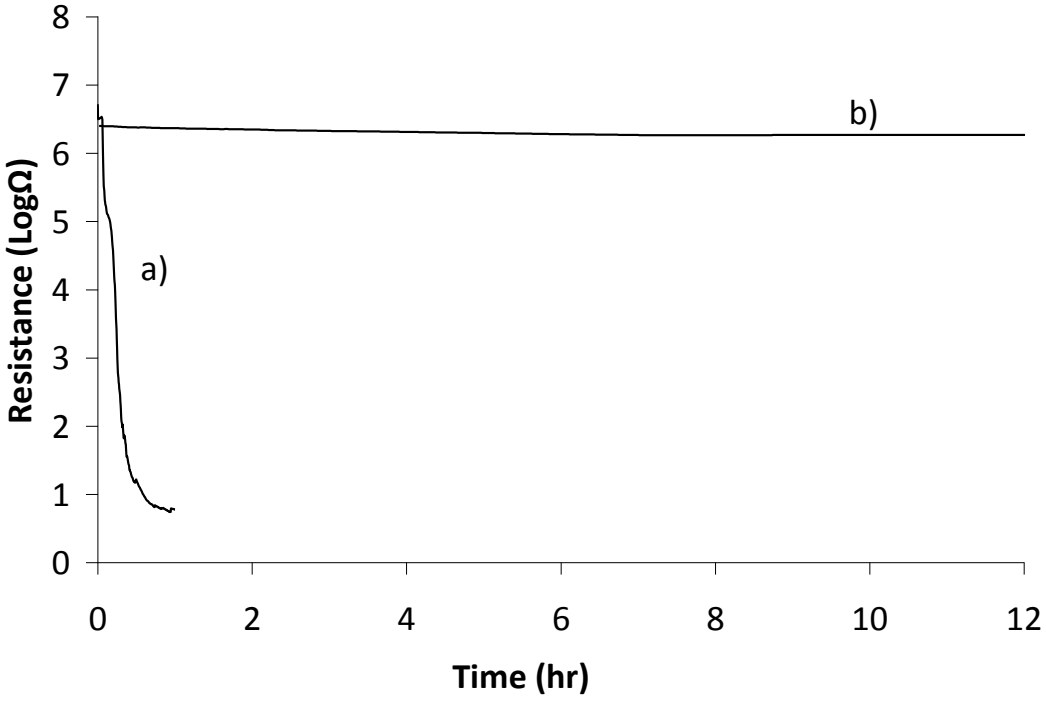

Figure 5. Resistance data for thin films of 1-butanethiol stabilized gold nanoparticles at room temperature under a stream of NO_2 gas, a), and in air, b).

Oxidation of sulphur atoms can readily occur when thiol-anchored self-assembled monolayers (SAMs) on gold are exposed to ordinary laboratory conditions for relatively short periods of time.[21] Oxidation reduces the thiol's ability to bind to gold and severely affects the SAM stability. We therefore examined the effect on sintering of exposing films of 1-butanethiol-stabilised gold nanoparticles to ambient conditions. Films aged in air were found to sinter more readily relative to freshly prepared samples (see Supporting Information), consistent with the effect of oxygen observed in previous experiments. We reasoned that the sintering rate should be increased further if nanoparticle films are exposed to strongly oxidizing atmospheres. Thus, nanoparticle films were exposed to nitrogen dioxide gas (which is capable of oxidising thiols[22]) at room temperature and the resistance measured. Figure 5 shows that a significant decrease in resistance occurs upon exposure to the oxidizing vapour and after 50 minutes the film resistance is consistent with that of sintered particles. A control experiment performed in air at room temperature shows that even after extended periods of time the resistance of the nanoparticles does not fall significantly compared to the resistance measured upon NO_2 exposure.

Conclusion

While temperature has long been known to be an important factor in the sintering of gold nanoparticle films, we have shown here that oxidation of the protective ligand and the exothermic reduction of surface area are also very important factors. This new knowledge can be exploited to produce sintered and conductive films even at room temperature.

Acknowledgement. We thank the Microstructural Analytical Unit, UTS, for technical support and Dr J. Kalman, UTS, for helpful discussions

Supporting Information Available. SEM images, sintering results for varying chain lengths and ambient exposure times, surface energy calculations, TGA data (PDF). This material is available free of charge via the Internet at http://pubs.acs.org.

References

1. Y. L. Wu, Y. N. Li, P. Liu, S. Gardner and B. S. Ong, *Chem. Mater.*, 2006, **18**, 4627-4632.
2. N. Zhao, M. Chiesa, H. Sirringhaus, Y. N. Li and Y. L. Wu, *J. Appl. Phys.*, 2007, **101**, 064513/1
3. S. H. Ko, H. Pan, C. P. Grigoropoulos, C. K. Luscombe, J. M. J. Frechet and D. Poulikakos, *Appl. Phys. Lett.*, 2007, **90**.
4. D. Huang, F. Liao, S. Molesa, D. Redinger and V. Subramanian, *J. Electrochem. Soc.*, 2003, **150**, G412-G417.
5. Y. Chen, R. E. Palmer and J. P. Wilcoxon, *Langmuir*, 2006, **22**, 2851-2855.
6. S. H. Ko, H. Pan, C. P. Grigoropoulos, C. K. Luscombe, J. M. J. Frechet and D. Poulikakos, *Nanotechnology*, 2007, **18**.
7. N. R. Bieri, J. Chung, S. E. Haferl, D. Poulikakos and C. P. Grigoropoulos, *Appl. Phys. Lett.*, 2003, **82**, 3529-3531.
8. J. Chung, S. Ko, N. R. Bieri, C. P. Grigoropoulos and D. Poulikakosa, *Appl. Phys. Lett.,*, 2004, **84**, 801-803.
9. S. Sun, P. Mendes, K. Critchley, S. Diegoli, M. Hanwell, S. D. Evans, G. J. Leggett, J. A. Preece and T. H. Richardson, *Nano Lett.*, 2006, **6**, 345-350.
10. V. Popescu, I. Vida-Simiti and N. Jumate, *Gold Bull.*, 2005, **38**, 163-169.
11. K. E. J. Lehtinen and M. R. Zachariah, *Phys. Rev. B*, 2001, **6320**.
12. K. E. J. Lehtinen and M. R. Zachariah, *J. Aerosol Sci.*, 2002, **33**, 357-368.
13. P. Buffat, *Phys. Rev. A*, 1976, **13**.
14. K. Dick, T. Dhanasekaran, Z. Zhang and D. Meisel, *J. Am. Chem. Soc.*, 2002, **124**, 2312-2317.
15. D. K. Breitinger and W. A. Herrmann, *Synthetic Methods of Organometallic and Inorganic Chemistry*, George Thieme Verlag, Stuttgart, 1999.
16. C. Duval, *Inorganic Thermogravimetric Analysis*, Elsevier, Amsterdam, 1963.
17. R. C. Hoft, N. Armstrong, M. J. Ford and M. B. Cortie, *J. Phys.: Condens. Matt.*, 2007, **19**, 215206.
18. R. J. Needs and M. Mansfield, *J. Phys.: Condens. Matt.*, 1989, **1**, 7555.
19. A. Savitzky and M. J. E. Golay, *Anal. Chem.*, 1964, **36**, 1627.
20. G. Yang, N. A. Amro, Z. B. Starkewolfe and G.-y. Liu, *Langmuir*, 2004, **20**, 3995-4003.
21. T. M. Willey, A. L. Vance, T. van Buuren, C. Bostedt, L. J. Terminello and C. S. Fadley, *Surf. Sci.*, 2005, **576**, 188-196.
22. W. A. Pryor, D. F. Church, C. K. Govindan and G. Crank, *J. Org. Chem.* 1982, **47**, 156-159.